



miR-106b-5p upregulation is associated with microglial activation and inflammation in the mouse hippocampus following status epilepticus

Tao Yu¹ · Hui Fu^{1,2} · Jing-Jing Sun¹ · Dan-Rui Ding¹ · Hua Wang¹

Received: 19 February 2021 / Accepted: 27 August 2021 / Published online: 2 September 2021
© The Author(s), under exclusive licence to Springer-Verlag GmbH Germany, part of Springer Nature 2021

Abstract

To investigate the association of miR-106b-5p with neuroinflammation and microglial activation in a status epilepticus (SE) mouse model. We examined changes in the expression of microRNA-106b-5p (miRNA-106b-5p), repulsive guidance molecule A (RGMa), triggering receptor expressed on myeloid cells 2 (TREM2), and the microglia-related markers interleukin (IL)-1 β , IL-4, IL-6, IL-10, inducible nitric oxide synthase (iNOS), and arginase-1 (Arg-1) in the mouse hippocampus of the lithium–pilocarpine-induced SE mouse model. Eighty-four female C57BL/6 mice were randomly divided into a normal control group ($n = 12$), and six SE groups ($n = 12$ /group), which were monitored at 6 h and at 1, 3, 7, 14, and 21 days (d) post-SE induction. Unlike in the dentate gyrus, immunohistochemical staining revealed prominent neuronal swelling at 6 h, significant neuronal loss and apoptosis on day 3, and recovery by day 14 in the hippocampal *cornu ammonis* (CA)1 and CA3 pyramidal cells in SE mice. We noted elevated levels of miRNA-106b-5p and all microglia-related markers, which peaked at 3 days post-SE, except IL-4, which peaked at 7 days post-SE, indicating inflammation and microglial activation. RGMa and TREM2 levels decreased at 6 h post-SE. All markers but miRNA-106b-5p, RGMa, and TREM2 returned to baseline levels at 21 days post-SE. Dual luciferase reporter gene assay showed that microRNA-106b-5p can interact with RGMa. We observed that miR-106b-5p level increased while both RGMa and TREM2 levels decreased post-SE and showed associations with microglial activation and inflammation in the mouse hippocampus, suggesting their potential as SE therapeutic targets.

Keywords miR-106b-5p · RGMa · TREM2 · Neuron · Microglia · Inflammation · Status epilepticus

Introduction

Epilepsy is a chronic brain disease characterized by aberrant, repetitive, and highly synchronized discharges of neurons, leading to seizures and potentially transient or permanent brain dysfunction (Upadhyaya et al. 2019). Active epilepsy has a point prevalence of 6.38 per 1000 people (Fiest et al.

2017) and a lifetime prevalence of 7.6 per 1000 people. According to the International League Against Epilepsy task force, status epilepticus (SE) is characterized by abnormally prolonged convulsive seizures lasting over 30 min that can lead to irreversible brain damage (Trinka et al. 2015). The primary treatment method for epilepsy at present is drug therapy, which is symptomatic and unable to curb disease progression. Approximately 30% of epilepsy patients are unresponsive to treatment and exhibit poor disease prognosis despite the development of alternative treatment options such as surgery, transcutaneous electrical nerve stimulation, and the ketogenic diet in recent years (Verrotti et al. 2020; Vezzani et al. 2011). Factors contributing to disease onset include genetics, central nervous system (CNS) infections and malignancies, and brain injury (Sirven 2015). As the underlying mechanism of epilepsy remains unclear, there is an imperative need to clarify and elucidate the disease pathogenesis to develop useful therapy options.

Communicated by Thomas Deller, M.D.

✉ Hua Wang
wangh1@sj-hospital.org

¹ Department of Pediatrics, Shengjing Hospital of China Medical University, China Medical University, No. 36, Sanhao Street, Heping District, Shenyang City 110004, Liaoning Province, China

² Department of Pediatrics, Tangshan Maternal and Child Health Care Hospital, Tangshan City 063000, Hebei Province, China

Microglial activation was found to be associated with SE, inducing the release of inflammatory mediators including interleukin (IL)-1 β , IL-6, tumor necrosis factor (TNF)- α , and reactive oxygen species (ROS), which lead to neuronal apoptosis and damage (Hiragi et al. 2018). Anti-inflammatory drugs such as steroid hormones and IL-1 β antagonists can also inhibit SE (Jin et al. 2019). Microglia are innate immune cells in the CNS that regulate homeostasis, synaptic activity, and neuronal apoptosis (Mosser et al. 2017; Voet et al. 2019). Forming part of the first-line innate immune response, microglia can switch from a physiological resting state (M0 type) to one of two pathological activated forms, specifically the classically activated M1-type or the alternative activated M2-type, which promotes inflammation and CNS damage (Schafer et al. 2013; Yu et al. 2019) and can lead to the development of neurodegenerative diseases (Walker and Lue 2015). The microglia activation marker triggering receptor expressed on myeloid cells 2 (TREM2) (Gisslén et al. 2019) was found to mediate the transition to disease-associated microglia in animal models of neurodegenerative diseases like Alzheimer's disease and amyotrophic lateral sclerosis (Da Mesquita and Kipnis 2017; Deming et al. 2018; Ulrich et al. 2017). Although TREM2 has been found to modulate immune cell survival, inflammation, and phagocytosis and its deficiency can lead to the manifestation of neurodegenerative pathologies (Deming et al. 2018; Jay et al. 2017), its role in disease pathogenesis remains unclear.

Although the etiology of epilepsy remains unclear, microRNAs (miRNAs) have been implicated in epilepsy and SE pathogenesis, specifically in processes including inflammation, apoptosis, and glial cell dysfunction (Brennan and Henshall 2020; Morris et al. 2019; Wang and Zhao 2021). Given the reported involvement of miRNA-106b-5p in microglial activation, microglial polarization, and inflammation following acute ischemic stroke and spinal cord injury (Li et al. 2017), as well as its upregulation in the peripheral blood of epilepsy patients (Wang et al. 2015), we examined its role in this study. Using miRNA analysis and target gene prediction programs, we identified repulsive guidance molecule A (RGMa) as the potential target gene of miRNA-106b-5p. RGMa regulates neural tube closure, neuronal survival, and neuronal differentiation, and guides axonal growth and regeneration following nerve injury by binding to its receptor protein neogenin (Siebold et al. 2017). Inhibiting RGMa could reduce CD4+ T-cell infiltration, the release of pro-inflammatory factors IL-2, IL-4, and interferon- γ , promote the recovery of nerve function in an autoimmune encephalomyelitis rat model (Muramatsu et al. 2011), and inhibit the secretion of TNF- α and IL-12 from dendritic cells (Xu et al. 2016). RGMa was also found to regulate axonal growth through microglia activation following spinal cord injury (Kitayama et al. 2011).

Currently, the associations of miR-106b-5p, RGMa, and TREM2 with microglial activation and phenotype switching following SE have not been characterized. Hence, we designed and performed this study to determine the roles of miR-106b-5p, RGMa, and TREM2 in microglial activation and polarization in mouse hippocampus following SE. SE animal models can be established through various methods including the administration of pilocarpine or kainic acid, or by electrical stimulation (Hiragi et al. 2018; Reddy and Kuruba 2013). We decided to use the lithium–pilocarpine induction method to establish the SE mouse model in this study (Liu et al. 2018; Müller et al. 2009; Shibley and Smith 2002). We examined the morphological changes and neuronal apoptosis in the mouse temporal lobe and hippocampus using techniques such as immunohistochemical staining, quantitative reverse transcription polymerase chain reaction (RT-qPCR), and western blot analyses. Our findings provide novel insights into the associations of miRNA-106b-5p with RGMa, TREM2, microglial activation, and inflammation in an SE mouse model, demonstrating the potential of these factors as molecular targets in SE therapy.

Materials and methods

Animal care and grouping

Eighty-four female C57BL/6 mice aged 8–10 weeks and weighing between 20 and 25 g were housed in a pathogen-free environment at ambient 20–24 °C conditions, under a standard 12 h light/dark cycle. Water and feed were provided ad libitum. The 84 mice were randomly divided into two groups: 12 in the control group and the remaining 72 in the SE model group. Animals in the SE model group were further divided into six groups ($n = 12$ /group) corresponding to the experimental time points of 6 h, 1 day, 3 days, 7 days, 14 days, and 21 days. For each group ($n = 12$), six animals were used for immunohistochemical and immunofluorescence staining, and six animals were used for RT-qPCR and western blot analyses. All animal experiments were performed according to the National Institutes of Health guidelines for the Care and Use of Laboratory Animals (NIH publication 80-23, revised in 1996) and the necessary approval (2020PS505K) was obtained from the Animal Ethics Committee of Shengjing Hospital Affiliated with China Medical University.

Establishment of an SE mouse model

We established the SE mouse model using previously described protocols (Liu et al. 2018; Müller et al. 2009; Shibley and Smith 2002). Mice in both SE and control groups were first injected with lithium chloride (127 mg/kg,

Sigma, USA) intraperitoneally, followed by bromomethyl scopolamine solution (1 mg/kg, Sigma, USA) after 16–18 h to minimize the pilocarpine-induced peripheral cholinergic response. Pilocarpine (96 mg/kg, Sigma, USA) was administered 30 min after the administration of scopolamine for the SE group. If no seizure occurred within 30 min or if the severity of the seizures was lower than stage 4 on the Racine behavioral scoring scale (Racine 1972), repeated pilocarpine doses (48 mg/kg; up to three supplementary injections) were administered till the mice exhibited persistent stage 4 epileptic seizures (characterized by seizures lasting over 30 min). The control group was injected with normal saline at the same dose as that for pilocarpine following the first two injections of lithium chloride and scopolamine. Mice exhibiting epileptic seizures lasting over 50 min were subjected to intraperitoneal diazepam (10 mg/kg) injection to terminate the seizures. After successful establishment of the SE mouse model, the animals in the SE group were sacrificed at 6 h, 1 day, 3 days, 7 days, 14 days, and 21 days after SE onset. Animals in the control group were sacrificed at the same time as the 21 days SE model group.

SE severity grading

The Racine behavioral scoring scale (Racine 1972), which ranges from stage 0 to 5, was used in the present study to assess the severity of epileptic behavior in the mice (Table 1).

Immunohistochemistry and hematoxylin and eosin (HE) staining

After SE onset, the mice were decapitated and brain hippocampal tissues were harvested at the following time points: 6 h, 1 day, 3 days, 7 days, 14 days, and 21 days. Mice in the normal control group ($n = 12$) were sacrificed at the 21-day time point. The mouse hippocampal brain tissue (4- μ m thick; six sections) was dehydrated, transparentized, paraffinized, and embedded, and then subjected to HE staining (staining with hematoxylin for 5 min and eosin for 3 min) to observe pathological changes in the hippocampal

tissue morphology after SE. HE-stained brain sections were visualized at $\times 200$ magnification using a BX53 optical microscope (Olympus). Images from three visual fields were randomly selected and captured for analyses.

Immunofluorescence

Neuronal nuclei antigen (NeuN) staining and the terminal deoxynucleotidyl transferase-mediated dUTP nick end labeling (TUNEL) assay were performed to assess the degree of neuronal loss and apoptosis, respectively, in the *cornu ammonis* (CA)1, CA3, and dentate gyrus (DG) regions of the mouse hippocampus after pilocarpine-induced SE. The paraffinized mouse brain tissue sections (six slices per group) were subjected to routine deparaffinization, hydration, transparentization, and antigen retrieval before labeling with the In Situ Cell Death detection kit (Roche, Switzerland) at 37 °C for 1 h. Antigen blocking was then performed and the sections were incubated with NeuN mouse monoclonal antibody (1:200 dilution, ab104224, Abcam, UK) at 4 °C overnight. The sections were subsequently incubated with Cy3 goat anti-mouse antibody (1:200 dilution, Biyuntian, China) at 4 °C overnight as well as with 4',6-diamidino-2-phenylindole (DAPI) reagent (Aladdin, China) at room temperature for 5 min. The stained mouse brain sections were visualized at $\times 400$ magnification using a DP73 fluorescence microscope (Olympus). Images from three visual fields were randomly selected and captured for analyses.

RT-qPCR

RT-qPCR was used to detect the expression of miRNA-106b-5p, RGMa, TREM2, and pro-inflammatory cytokines IL-1 β , IL-4, IL-6, and IL-10 in the microglia in the mouse hippocampus following SE. Microglial activation and M0 to M1/M2 switching following SE were also assessed through inducible nitric oxide synthase (iNOS) and arginase-1 (Arg-1) detection. Total RNA was extracted from the mouse hippocampus using the RNAsimple Total RNA kit (Tiangen, China). Reverse transcription using the BIONEER Exicycler™ 96 Real-Time Quantitative Thermal Blocksystem was

Table 1 Racine scale

Stage	Behavior
Stage 0	No changes in movement and behavior
Stage 1	Abnormal facial movements including excessive blinking, twitching of the whiskers, rhythmic chewing, and wet dog shakes (rapid alternating head rotations)
Stage 2	Head nodding due to uncontrollable neck muscle contractions
Stage 3	Involuntary forelimb movement and shaking
Stage 4	Involuntary shaking of the sides and forelimbs accompanied by rearing movements
Stage 5	Rearing and falling, excessive forelimb movement, sustained standing and falling, imbalance, and generalized motor convulsions

performed to synthesize cDNA, which was subsequently used in the PCR reaction. PCR was conducted using the PCR amplification kit with 2×Taq PCR Mastermix (Tiangen, China) and Solarbio SYBR Green dye (Solarbio, China). The following PCR reaction conditions were used: *miRNA*: 94 °C for 2 min, 94 °C for 15 s, 60 °C for 15 s, 72 °C for 15 s, amplification for 40 cycles; *mRNA*: 94 °C for 5 min, 94 °C for 10 s, 60 °C for 20 s, 72 °C for 30 s, amplification for 40 cycles. The sequences for the primers used in PCR were as follows: *miR-106b-5p*: for, 5'-TAAAGTGCTGACAGTGCAGAT-3', rev, 5'-GCAGGGTCCGAGGTATTC-3'; *IL-1β*: for, 5'-CTCAACTGTGAAATGCCACC-3', rev, 5'-GAGTGATACTGCCTGCCTGA-3'; *IL-4*: for, 5'-CATCCTGCTCTTCTTTCTCG-3', rev, 5'-CCTTCTCCTGTGACCTCGTT-3'; *IL-6*: for, 5'-ATGGCAATTCTGATTGATG-3', rev, 5'-GACTCTGGCTTTGTCTTTCT-3'; *IL-10*: for, 5'-TTAAGGGTTACTTGGGTTGC-3', rev, 5'-GAGGGTCTTCAGCTTCTCAC-3'; *RGMa*: for, 5'-CTTCCGTCTGCCTTTGCG-3', rev, 5'-CGATGGTGGTGCCGATGT-3'; *TREM2*: for, 5'-TGAAGAAGCGGAATGGG-3', rev, 5'-AGGTGGGTGGGAAGGAG-3'; *Glyceraldehyde-3-Phosphate Dehydrogenase (GAPDH)*: for, 5'-TGTTCCATCCCCAATGTGTCCGTC-3', rev, 5'-CTGGTCTCAGTGTAGCCCAAGATG-3'. Relative quantification was performed using the $2^{-\Delta\Delta ct}$ method and GAPDH was used as the internal normalization control.

Western blot analysis

Western blot analysis was performed to assess the RGMa and TREM2 levels in the mouse hippocampus following SE as well as to detect the expression of the polarization state markers for M1/M2-type microglia, iNOS and Arg-1, in the mouse hippocampus. Total protein was isolated from the brain hippocampal tissue lysate using radioimmunoprecipitation assay (RIPA) lysis buffer (Solarbio, China). Protein concentration was quantified using the bicinchoninic acid (BCA) assay (Solarbio, China) and proteins were separated with sodium dodecyl sulfate polyacrylamide gel electrophoresis (SDS-PAGE). The protein bands were subsequently transferred onto polyvinylidene fluoride membranes, which were first probed with RGMa, iNOS, or Arg-1 (1:1000 dilution, RGMa: DF13622, iNOS: AF0199, Arg-1: DF6657, Affinity, USA), or TREM2 (1:1000 dilution, A10482, Abclonal, China) rabbit primary antibodies at 4 °C overnight. The membranes were subsequently incubated with goat anti-rabbit or anti-mouse horse radish peroxidase (HRP)-conjugated secondary antibody (1:5000 dilution, anti-rabbit: SE134, anti-mouse: SE131, Solarbio, China) for 1 h at room temperature. Protein bands were then visualized using an enhanced chemiluminescence reagent (Solarbio, China) and the band intensities were analyzed using the Gel-Pro-Analyzer software (Media Cybernetics, USA). GAPDH

(60004-1-Ig, Proteintech, China) was used as the internal normalization control.

Dual luciferase reporter gene assay

The pmirGLO plasmids containing the firefly luciferase gene and wild-type (RGMa-wt) or mutant (RGMa-mut) fragments of the RGMa 3'-untranslated region (UTR) with the predicted miR-106b-5p binding site were transfected into human embryonic kidney (HEK)293T cells. The binding site was predicted using the miRNA analysis and target gene prediction programs miRNAwalk (Sticht et al. 2018) and TargetScan (http://www.targetscan.org/vert_72/). The transfection reagent was used for transfection of the plasmids into HEK293T cells in Dulbecco's Modified Eagle's medium (DMEM) and cultured at 37 °C for 48 h in a 5% CO₂ humidified incubator. The plasmid containing the negative control miRNA mimic was used as a transfection control. The transfected cells were harvested after 48 h and luciferase activity was measured using the Dual-Luciferase[®] Reporter Assay System (Promega, Madison, WI, USA). The firefly luciferase activity of each sample was normalized against Renilla luciferase activity. Three independent experiments were performed.

Statistical analysis

Statistical analysis was performed using the GraphPad Prism 8.0 software. All data were expressed as the mean ± standard deviation (SD). Comparisons among groups were performed using one-way analysis of variance (ANOVA). Values of $P < 0.05$ were deemed statistically significant.

Results

Successful establishment of SE mouse model

Animals that failed to reach at least stage 4 epileptic seizures or died before successful model establishment were replaced with new animals to give a final total number of 72 successful pilocarpine-induced SE mice. After administering the first dose of pilocarpine, all mice showed stage 1 SE with symptoms of seizures and tremors at 15.3 ± 1.2 min, which gradually worsened. Repeated dosing with pilocarpine caused 90.7% (78/86) of the mice to develop stage 4–5 seizures. Mice with stage 4 and above sustained seizures lasting 50 min were treated with diazepam intraperitoneally to stop the convulsions. Out of 78 animals, 75 received diazepam. The three animals that did not receive diazepam had convulsions lasting < 50 min. Convulsions gradually stopped after 2 ± 0.6 h (mean overall seizure duration for all 78 mice). Mice with convulsions that could not be controlled by

diazepam eventually died and were replaced with successfully modeled animals (6/86). Discounting the six mice that died after nearly 4 h of convulsions, the overall mean seizure duration for the remaining 72 mice was 108.5 ± 23.7 min.

SE causes neuronal damage in the CA1 and CA3 regions of the mouse hippocampus

We assessed the histopathological changes in the morphology and structure of the CA1 and CA3 pyramidal cells and the DG regions of the mouse hippocampus after pilocarpine-induced SE by HE staining (Fig. 1A–D). Compared with the control group (Fig. 1Aa1, 2), the CA1 and CA3 regions of the SE mouse hippocampus showed

uneven staining in the cytoplasm and nucleus, indicative of less defined morphology and neuronal swelling at 6 h after SE induction (Fig. 1Ab1, 2). More intense staining of the nuclei and cytoplasm, prominent loss of pyramidal cells, decreased neuronal volume, and shrunken nuclei and indistinct nucleoli were observed 3 days after SE induction (Fig. 1Ad1, 2, B–C). Slight alleviation of the SE symptoms was noted on day 7 after SE induction, with a slight recovery in the number of pyramidal cells (Fig. 1Ae1, 2, B–C). The recovery continued on days 14 and 21 after SE with more uniform staining of the nuclei and cytoplasm, and the morphology of the pyramidal cells was eventually restored (Fig. 1Af1, 2, g1, 2). No significant changes in the histopathology of granule cells in the hippocampal DG region were observed (Fig. 1Aa3–g3, D).

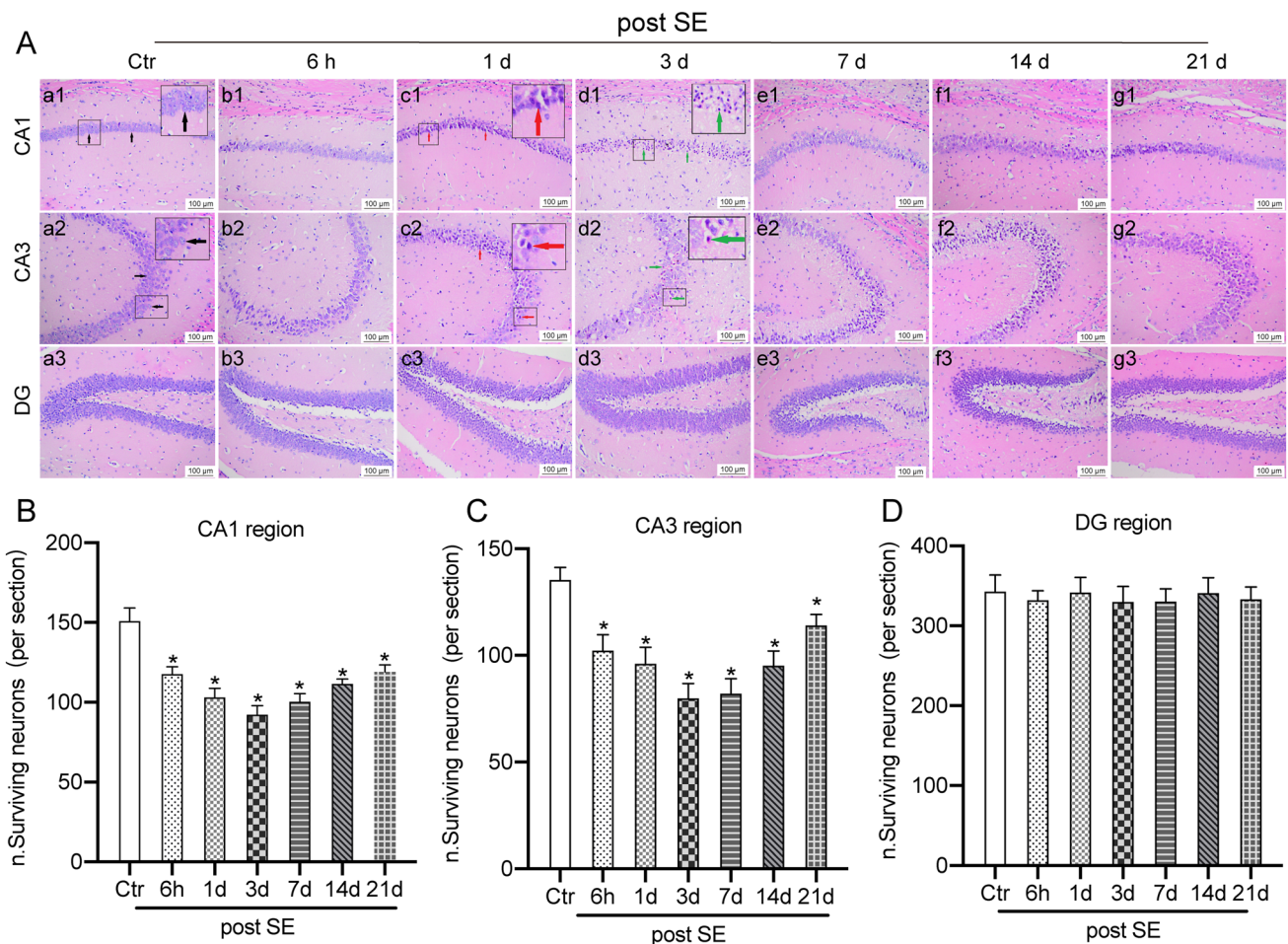


Fig. 1 A HE immunohistochemical staining images of mouse hippocampus CA1, CA3, and DG regions of (a1-3) normal control group and SE groups at (b1-3) 6 h (6 h), (c1-3) 1 day (1d), (d1-3) 3 days (3d), (e1-3) 7 days (7d), (f1-3) 14 days (14d), and (g1-3) 21 days (21d) post-SE at $\times 200$ magnification. Black arrows: normal neurons;

red arrows: shrunken neurons, intensely stained cytoplasm; green arrows: smaller neuronal cell body and shrunken nucleus (pyknosis). Semi-quantitative histograms of HE staining images of mouse hippocampus **B** CA1, **C** CA3, and **D** DG regions of normal control group and SE groups

Neuronal apoptosis and neurodegeneration occur after SE onset

Immunohistochemistry was employed to assess changes in the neuronal numbers in the CA1, CA3, and DG regions of the mouse hippocampus of the SE and normal control groups (Fig. 2A–D). Decreased NeuN staining was observed in the CA1 and CA3 regions of the mouse hippocampus on day 3 after SE (Fig. 2Ab1, Ae1, E, F), indicating neuronal loss, but the NeuN level was restored on day 7 after SE, and was comparable to that for the day 3 mouse (Fig. 2a1–f1, E–F). No significant changes were observed from NeuN staining of the DG region of the mouse hippocampus post-SE (Fig. 2Ag1–i1, G). TUNEL assay revealed the occurrence

of neuronal cell apoptosis in the CA1 and CA3 regions of the mouse hippocampus at 6 h and days 1, 3, and 7 after SE induction, especially on day 3, but no apoptotic cells were noted on days 14 and 21 post-SE (Fig. 2B, Da4–f4, H, I and Supp. Fig. 1). No apoptotic cells were found in both the normal and SE mouse hippocampal DG regions (Fig. 2Dg4–i4).

miRNA-106b-5p level is upregulated while RGMA and TREM2 levels are downregulated post-SE

RT-qPCR revealed elevated levels of miRNA-106b-5p, M1-type microglia markers IL-1 β and IL-6, and M2-type microglia markers IL-4 and IL-10 in mouse hippocampus in general, but decreased RGMA and TREM2 levels over

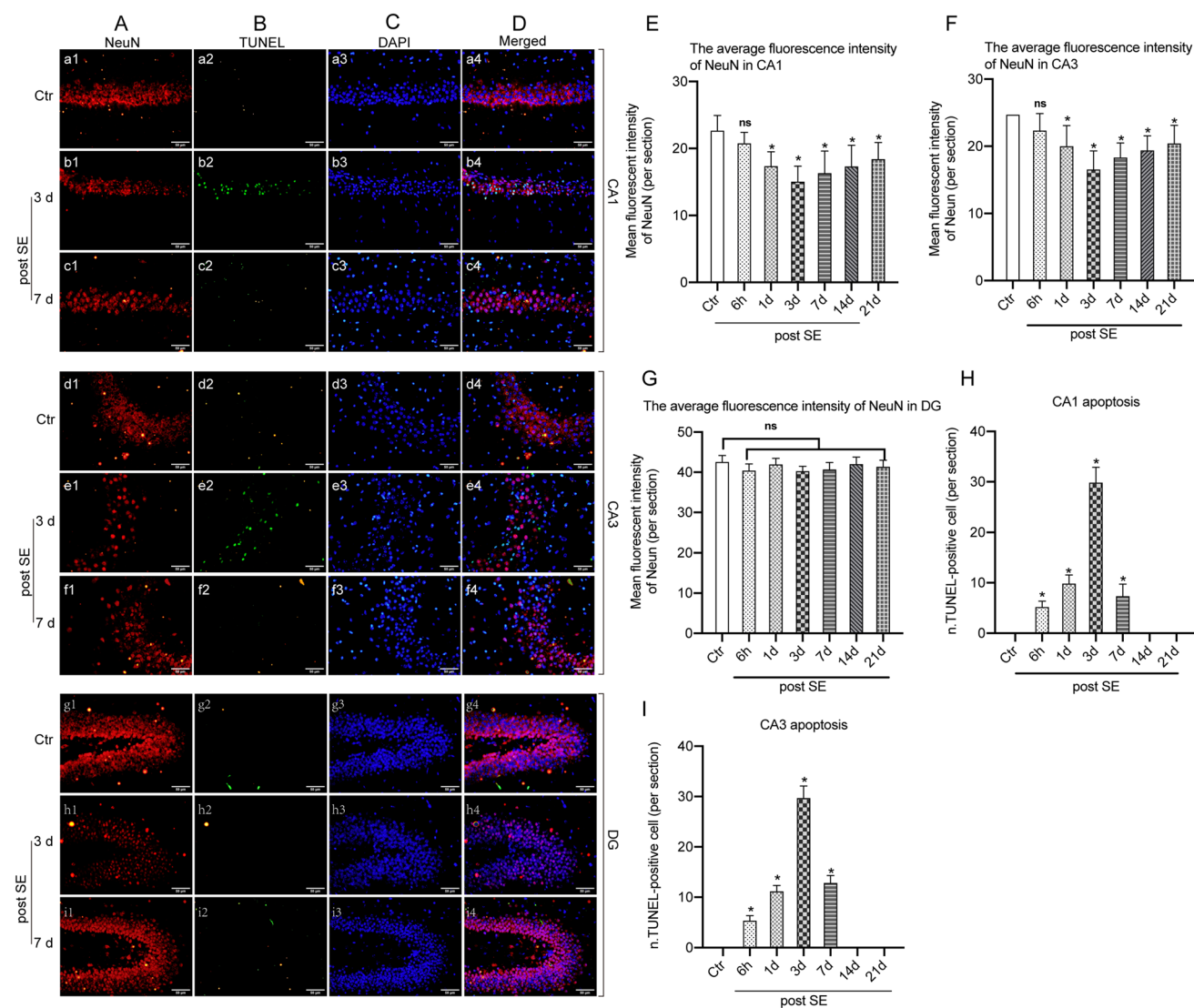


Fig. 2 A (a1–i1) NeuN, B (a1–i1) TUNEL, C (a1–i1) DAPI, and D (a1–i1) merged immunohistochemical staining images of mouse hippocampus CA1, CA3, and DG regions of normal control group and SE group at 3 (3d) and 7 (7d) days post-SE at $\times 400$ magnification.

E–I Semi-quantitative histograms of NeuN-positive cells in **E** CA1, **F** CA3 and **G** DG regions, and TUNEL-positive apoptotic cells in **H** CA1 and **I** CA3 regions

the 21-day post-SE period compared with the levels in the control group ($P < 0.05$; Fig. 3A–G and Supp. Figs. 2 and 3). Notably, miRNA-106b-5p, IL-1 β , IL-6, and IL-10 levels peaked on day 3 post-SE, while the IL-4 level peaked on day 7 post-SE. The IL-1 β , IL-4, IL-6, and IL-10 levels returned to the baseline level at 21 days post-SE but the miRNA-106b-5p level remained elevated ($P < 0.05$; Fig. 3A, D–G). Next, we performed western blot analysis to determine the levels of RGMA, TREM2, the M1-type microglia marker iNOS, and the M2-type microglia marker Arg-1. Downregulated RGMA and TREM2 protein levels in SE mouse compared with the levels in normal control mouse observed in the western blot results (Fig. 4) were consistent with the RT-qPCR results (Fig. 4). Both the western blot and RT-qPCR results were in line with the neuronal loss observed from NeuN immunohistochemical staining (Fig. 2). We observed increased iNOS and Arg-1 protein levels in the SE group compared with the levels in the normal control group, with peak protein levels at 3 days post-SE and recovery to baseline levels at 21 days post-SE (Fig. 4).

miR-106b-5p interacts with RGMA

Using the miRNAwalk and TargetScan gene target and binding site prediction programs, we identified RGMA as a target of miR-106b-5p and also predicted the miR-106b-5p binding site on RGMA (Fig. 5A). We performed a dual luciferase reporter assay to assess whether miR-106b-5p can interact with RGMA. Lower luciferase signal intensity was observed in HEK293T cells co-transfected with the miR-106b-5p mimic and RGMA-wt, while no significant change

in luciferase activity was observed in the cells co-transfected with the miR-106b-5p mimic and RGMA-mut (Fig. 5B; $P < 0.001$). These results confirmed the interaction between miR-106b-5p and RGMA, and that the former represses the latter’s expression.

Discussion

After establishing the SE mouse model via lithium–pilocarpine induction, we selected mice diagnosed with SE higher than stage 4 on the Racine scale for subsequent experiments. Activated microglia (M1- and M2-types) have been implicated in disease pathogenesis and are reportedly associated with epilepsy (Hiragi et al. 2018; Schafer et al. 2013; Yu et al. 2019). SE mice exhibited increased neurodegeneration, apoptosis, and inflammation, and elevated M1- and M2-type microglia, indicating microglial activation in the hippocampal CA1 and CA3 regions 6 h after SE onset but recovered by 21 days after SE onset. Consistent with previous observations (Reddy and Kuruba 2013), we also noted neuronal apoptosis in the hippocampal CA1 and CA3 regions post-SE, with the most significant decrease at the day 3 time point. Although there was a slight recovery in later periods, the number of neurons still could not compare to that of the control group. We speculate that the slight recovery in the number of neurons at the CA1 and CA3 regions is related to neurogenesis after injury. Although we did not detect neurogenesis in this study, neurogenesis in the CA1 area after ischemic brain injury has been reported (Nakatomi et al. 2002). Although hyperplasia of the granule cells in the DG

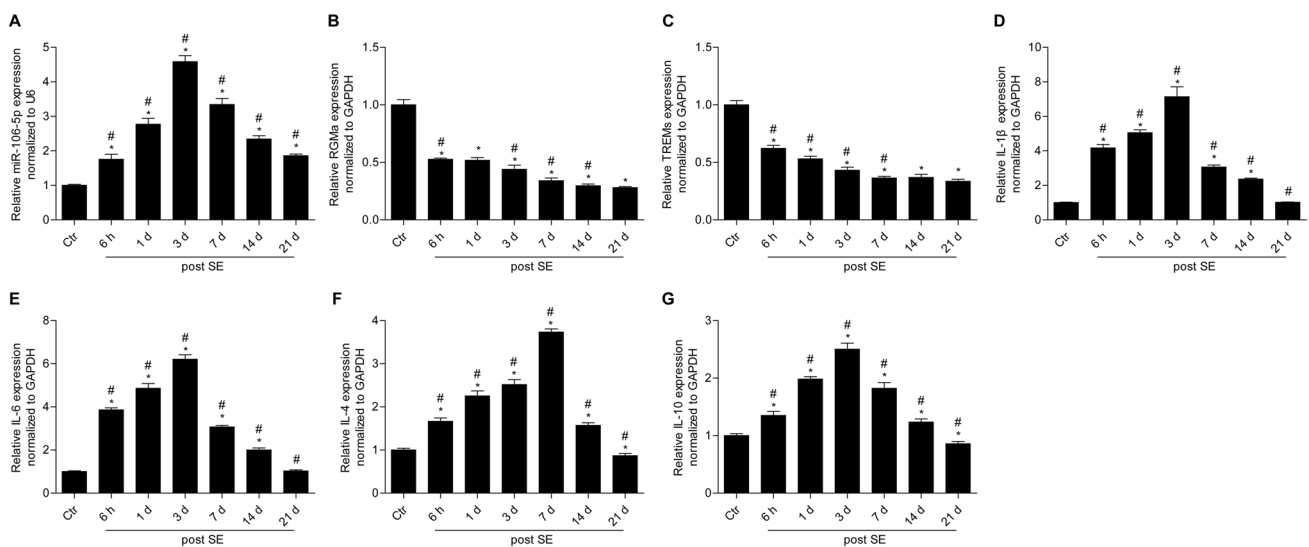


Fig. 3 RT-qPCR profiles of the expression of **A** miR-106b-5p and **B** RGMA, **C** TREM2, **D** IL-1 β , **E** IL-4, **F** IL-6, and **G** IL-10 mRNA in the mouse hippocampus of the normal control group and SE group at 6 h (6h), 1 day (1d), 3 days (3d), 7 days (7d), 14 days (14d), and

21 days (21d) following SE. Relative GAPDH mRNA expression was used as the internal normalization control. Data for the average of three independent experiments are shown. * $P < 0.05$ vs control; # $P < 0.01$ vs the preceding group compared

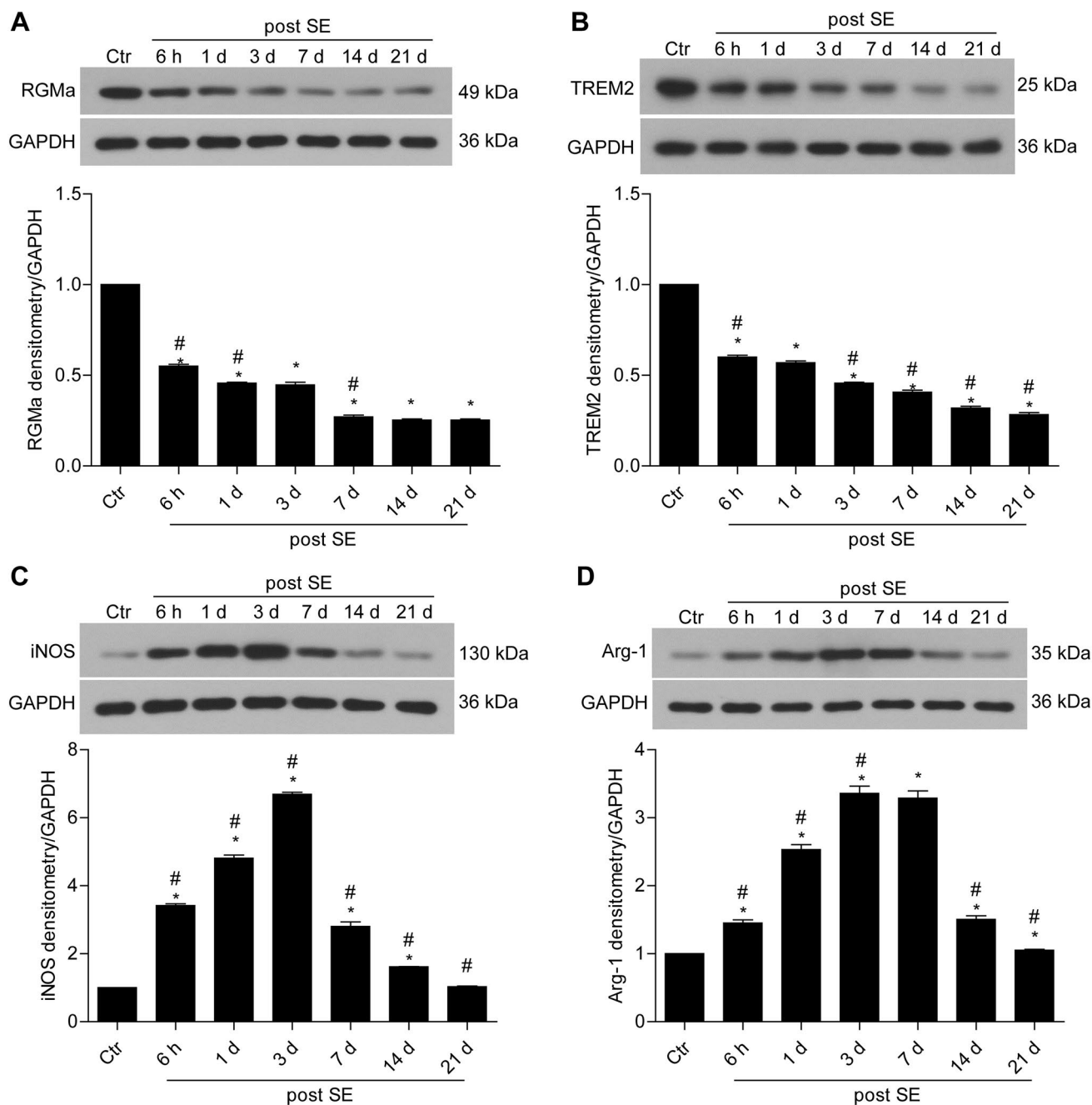


Fig. 4 Western blot images and corresponding histograms of the protein levels of **A** RGMa, **B** TREM2, **C** iNOS, and **D** Arg-1 in the mouse hippocampus of the normal control group and SE group at 6 h (6h), 1 day (1d), 3 days (3d), 7 days (7d), 14 days (14d), and 21 days

(21d) following SE. Relative GAPDH protein expression was used as the internal normalization control. Data for the average of three independent experiments are shown

has been reported (Luo et al. 2016), these cells could not be detected with HE and TUNEL staining, thus explaining the lack of changes in the DG observed in this study. Doublecortin labeling could be performed in a follow-up study to confirm the effect on immature granule cells in the DG. RT-qPCR and western blot analyses revealed elevated miRNA-106b-5p levels but decreased RGMa and TREM2

levels in SE mouse compared with those in normal control mouse. Notably, the peak levels of miRNA-106b-5p and the M1-type and M2-type microglia markers were associated with increased neuronal loss in mouse hippocampus at 3 days post-SE. These results indicate that miRNA-106b-5p is correlated with microglial activation and polarization, inflammation, and neurodegeneration. The dual luciferase

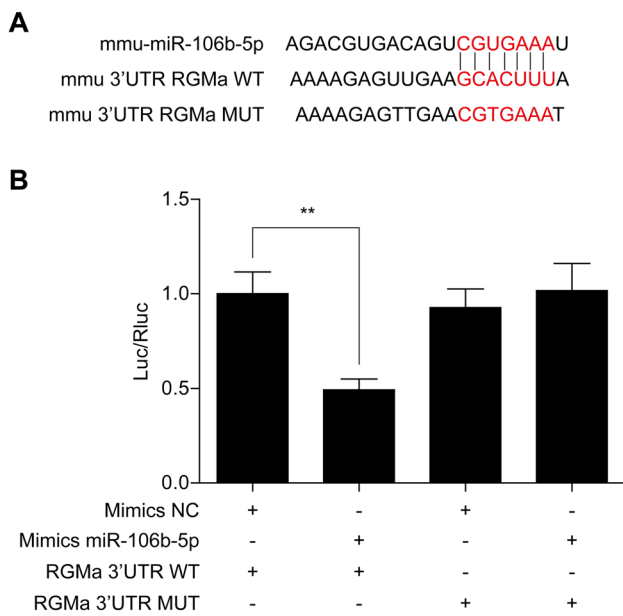


Fig. 5 miRNA-106b-5p can bind to and repress RGMa expression. **A** RGMa 3'-UTR wild-type (RGMa-wt) sequence containing the miRNA-106b-5p binding site and sequence of the mutant (RGMa-mut) miRNA-106b-5p binding site. Luciferase reporter gene assay (images and histograms) showed lower luciferase activity for **B** miRNA-106b-5p and RGMa-wt than for RGMa-mut ($P < 0.05$). Data for the average of three independent experiments are shown. One-way ANOVA was performed for comparisons between two groups. $**P < 0.001$

reporter gene assay confirmed the inverse correlation between miRNA-106b-5p and RGMa levels and demonstrated that the former could inhibit the expression of the latter. Given the varied roles of miRNAs in important biological processes, they have been proposed to be biomarkers and therapeutic targets for epilepsy (Brennan and Henshall 2020; Wang and Zhao 2021) and SE (Brindley et al. 2019). Our results suggest the association of miRNA-106b-5p with microglial activation and inflammation following SE and propose miRNA-106b-5p and RGMa as potential diagnostic SE biomarkers and molecular targets in SE therapy.

Chronic microglial activation and polarization can result in the secretion of pro-inflammatory factors, leading to excessive neuronal excitation and neuronal damage, thereby promoting epilepsy development (Hiragi et al. 2018; Therajaran et al. 2020). Switching from the pro-inflammatory M1-type to the anti-inflammatory M2-type microglia can prevent SE (Therajaran et al. 2020). Consistent with previous reports (Benson et al. 2015; Hiragi et al. 2018), we noted increased levels of both the pro-inflammatory M1-type cytokines IL-1 β , IL-6, and iNOS, and the anti-inflammatory M2-type cytokines IL-4, IL-10, and Arg-1. Elevation of both pro- and anti-inflammatory cytokines suggests the complex role of microglia in regulating inflammation in SE. We speculate that the upregulation of the competing

pro-inflammatory M1-type microglial marker iNOS and anti-inflammatory M2-type microglia marker Arg-1 could be due to the increase in both M1- and M2-type microglia (Avignone et al. 2008). In addition, we also speculate that inflammation-induced negative feedback might have resulted in the increase in M2-type microglial markers Arg-1 and IL-4 levels (Arg-1 and IL-4 levels peak later than iNOS, IL-1, and IL-6 levels). TREM2's role in microglia activation (Gisslén et al. 2019) is contradictory to its anti-inflammatory role (Jay et al. 2017), further demonstrating the complex role of disease-associated microglia. This complexity could also be attributed to the association between M1/M2 phenotypic switching and multiple signaling pathways (Jin et al. 2019). The proportion of M1/M2-type microglia could be determined using flow cytometry in a follow-up study to clarify the role of microglia polarization in SE.

TREM2 has been shown to inhibit neuronal apoptosis (Liu et al. 2019) and inflammation (Jiang et al. 2018; Liu et al. 2020). RGMa has also been shown to inhibit seizures in epilepsy animal models (Müller et al. 2009). These findings were consistent with our observations of downregulated RGMa and TREM2 mRNA and protein levels as well as neuronal loss in SE mice in this study. Interestingly, the miRNA-106b-5p, RGMa, and TREM2 levels in SE mice failed to recover to baseline levels by day 21 post-SE onset unlike the levels of the microglia-related factors, possibly indicating other modulatory factors at play. This may in part be influenced by the complex role of microglia in SE. Including longer time points in the study design with a larger sample size could facilitate better insights into whether the miRNA-106b-5p, RGMa, and TREM2 levels can be restored to baseline levels in an SE model. This could potentially be explored in future follow-up studies.

SE animal models can be established with the injection of chemical convulsants such as pilocarpine and kainic acid or by electrical stimulation of regions of the brain to induce convulsions (Hiragi et al. 2018). Using a combination of lithium and pilocarpine has been shown to reduce the pilocarpine threshold dose required to induce SE, thereby reducing the animal mortality rate and enabling a higher model establishment success rate (Song et al. 2019). As experimental animals have been found to exhibit variable sensitivity to kainic acid, and SE model creation by electrical stimulation requires expensive equipment (Reddy and Kuruba 2013), we chose the lithium–pilocarpine induction method to establish our SE mouse model in this study. Nonetheless, the findings of this study should be confirmed with other SE animal models in future studies to account for intrinsic differences in animal sensitivity to pilocarpine and mortality (Gupta et al. 2019), as well as SE neuropathology between different animal models that could affect microglial activation and polarization (Reddy and Kuruba 2013). In addition, we focused on examining the post-SE pathology in this study;

thus, the underlying mechanism of epileptogenesis could be another potential area worth exploring in future research.

In conclusion, we report for the first time that miR-106b-5p can regulate and interact with RGMA and that expression of the former was associated with microglial activation and inflammation in pilocarpine-induced SE mice. Elevated miR-106b-5p levels observed through RT-qPCR in this study were consistent with increased miR-106b serum levels in epilepsy patients in previous reports (An et al. 2016; Wang et al. 2015). Targeting miR-106b-5p-mediated inhibition of RGMA could represent a potential approach in SE clinical therapy but the findings in this study should first be confirmed with other animal models of SE. Given that TREM2 exhibited a similar expression profile as that of RGMA post-SE, miR-106b-5p could potentially inhibit TREM2 in a similar manner as RGMA. Future follow-up experiments would be needed to confirm the relationship between miR-106b-5p and TREM2.

Supplementary Information The online version contains supplementary material available at <https://doi.org/10.1007/s00221-021-06208-3>.

Acknowledgements None.

Author contributions HW and TY conceived and designed research; TY, HF and DRD collected data and conducted research; TY and JJS analyzed and interpreted data; TY wrote the initial paper; HW revised the paper; HW had primary responsibility for the final content. All authors read and approved the final manuscript.

Funding This work was supported by the National Key Research and Development Plan (Grant No. 2016YFC1306203).

Availability of data and material The datasets generated and analyzed during the current study are available from the corresponding author on reasonable request.

Declarations

Conflict of interest The authors declare that they have no conflicts of interest.

Ethical approval All animal experiments were performed according to the National Institutes of Health guidelines for the Care and Use of Laboratory Animals (NIH publication 80-23, revised in 1996) and the necessary approval (2020PS505K) was obtained from the Animal Ethics Committee of Shengjing Hospital Affiliated with China Medical University.

Consent to participate Not applicable.

Consent for publication Not applicable.

References

An N, Zhao W, Liu Y, Yang X, Chen P (2016) Elevated serum miR-106b and miR-146a in patients with focal and generalized

epilepsy. *Epilepsy Res* 127:311–316. <https://doi.org/10.1016/j.epilepsyres.2016.09.019>

Avignone E, Ulmann L, Levavasseur F, Rassendren F, Audinat E (2008) Status epilepticus induces a particular microglial activation state characterized by enhanced purinergic signaling. *J Neurosci* 28:9133–9144. <https://doi.org/10.1523/jneurosci.1820-08.2008>

Benson MJ, Manzanero S, Borges K (2015) Complex alterations in microglial M1/M2 markers during the development of epilepsy in two mouse models. *Epilepsia* 56:895–905. <https://doi.org/10.1111/epi.12960>

Brennan GP, Henshall DC (2020) MicroRNAs as regulators of brain function and targets for treatment of epilepsy. *Nat Rev Neurol* 16:506–519. <https://doi.org/10.1038/s41582-020-0369-8>

Brindley E, Hill TDM, Henshall DC (2019) MicroRNAs as biomarkers and treatment targets in status epilepticus. *Epilepsy Behav* 101:106272. <https://doi.org/10.1016/j.yebeh.2019.04.025>

Da Mesquita S, Kipnis J (2017) DAMed in (Trem) 2 steps. *Cell* 169:1172–1174. <https://doi.org/10.1016/j.cell.2017.05.039>

Deming Y, Li Z, Benitez BA, Cruchaga C (2018) Triggering receptor expressed on myeloid cells 2 (TREM2): a potential therapeutic target for Alzheimer disease? *Expert Opin Ther Targets* 22:587–598. <https://doi.org/10.1080/14728222.2018.1486823>

Fiest KM, Sauro KM, Wiebe S, Patten SB, Kwon CS, Dykeman J, Pringsheim T, Lorenzetti DL, Jetté N (2017) Prevalence and incidence of epilepsy: a systematic review and meta-analysis of international studies. *Neurology* 88:296–303. <https://doi.org/10.1212/wnl.0000000000003509>

Gisslén M, Heslegrave A, Veleva E, Yilmaz A, Andersson LM, Hagberg L, Spudich S, Fuchs D, Price RW, Zetterberg H (2019) CSF concentrations of soluble TREM2 as a marker of microglial activation in HIV-1 infection. *Neurol Neuroimmunol Neuroinflamm* 6:e512. <https://doi.org/10.1212/wnxi.0000000000000512>

Gupta J, Bromwich M, Radell J, Arshad MN, Gonzalez S, Luikart BW, Aaron GB, Naegel JR (2019) Restrained dendritic growth of adult-born granule cells innervated by transplanted fetal GABAergic interneurons in mice with temporal lobe epilepsy. *eNeuro*. <https://doi.org/10.1523/eneuro.0110-18.2019>

Hiragi T, Ikegaya Y, Koyama R (2018) Microglia after seizures and in epilepsy. *Cells*. <https://doi.org/10.3390/cells7040026>

Jay TR, von Saucken VE, Landreth GE (2017) TREM2 in neurodegenerative diseases. *Mol Neurodegener* 12:56. <https://doi.org/10.1186/s13024-017-0197-5>

Jiang Y, Li Z, Ma H, Cao X, Liu F, Tian A, Sun X, Li X, Wang J (2018) Upregulation of TREM2 ameliorates neuroinflammatory responses and improves cognitive deficits triggered by surgical trauma in Apswe/PS1dE9 Mice. *Cell Physiol Biochem* 46:1398–1411. <https://doi.org/10.1159/000489155>

Jin X, Liu MY, Zhang DF, Zhong X, Du K, Qian P, Gao H, Wei MJ (2019) Natural products as a potential modulator of microglial polarization in neurodegenerative diseases. *Pharmacol Res* 145:104253. <https://doi.org/10.1016/j.phrs.2019.104253>

Kitayama M, Ueno M, Itakura T, Yamashita T (2011) Activated microglia inhibit axonal growth through RGMA. *PLoS ONE* 6:e25234. <https://doi.org/10.1371/journal.pone.0025234>

Li P, Shen M, Gao F, Wu J, Zhang J, Teng F, Zhang C (2017) An antagonist to microRNA-106b-5p ameliorates cerebral ischemia and reperfusion injury in rats via inhibiting apoptosis and oxidative stress. *Mol Neurobiol* 54:2901–2921. <https://doi.org/10.1007/s12035-016-9842-1>

Liu JT, Wu SX, Zhang H, Kuang F (2018) Inhibition of MyD88 signaling skews microglia/macrophage polarization and attenuates neuronal apoptosis in the hippocampus after status epilepticus in mice. *Neurotherapeutics* 15:1093–1111. <https://doi.org/10.1007/s13311-018-0653-0>

Liu AH, Chu M, Wang YP (2019) Up-regulation of Trem2 inhibits hippocampal neuronal apoptosis and alleviates oxidative stress

- in epilepsy via the PI3K/Akt pathway in mice. *Neurosci Bull* 35:471–485. <https://doi.org/10.1007/s12264-018-0324-5>
- Liu W, Taso O, Wang R et al (2020) Trem2 promotes anti-inflammatory responses in microglia and is suppressed under pro-inflammatory conditions. *Hum Mol Genet* 29:3224–3248. <https://doi.org/10.1093/hmg/ddaa209>
- Luo C, Koyama R, Ikegaya Y (2016) Microglia engulf viable newborn cells in the epileptic dentate gyrus. *Glia* 64:1508–1517. <https://doi.org/10.1002/glia.23018>
- Morris G, Reschke CR, Henshall DC (2019) Targeting microRNA-134 for seizure control and disease modification in epilepsy. *EBio-Medicine* 45:646–654. <https://doi.org/10.1016/j.ebiom.2019.07.008>
- Mosser CA, Baptista S, Arnoux I, Audinat E (2017) Microglia in CNS development: shaping the brain for the future. *Prog Neurobiol* 149–150:1–20. <https://doi.org/10.1016/j.pneurobio.2017.01.002>
- Müller CJ, Bankstahl M, Gröticke I, Löscher W (2009) Pilocarpine vs. lithium-pilocarpine for induction of status epilepticus in mice: development of spontaneous seizures, behavioral alterations and neuronal damage. *Eur J Pharmacol* 619:15–24. <https://doi.org/10.1016/j.ejphar.2009.07.020>
- Muramatsu R, Kubo T, Mori M et al (2011) RGMA modulates T cell responses and is involved in autoimmune encephalomyelitis. *Nat Med* 17:488–494. <https://doi.org/10.1038/nm.2321>
- Nakatomi H, Kuriu T, Okabe S, Yamamoto S, Hatano O, Kawahara N, Tamura A, Kirino T, Nakafuku M (2002) Regeneration of hippocampal pyramidal neurons after ischemic brain injury by recruitment of endogenous neural progenitors. *Cell* 110:429–441. [https://doi.org/10.1016/s0092-8674\(02\)00862-0](https://doi.org/10.1016/s0092-8674(02)00862-0)
- Racine RJ (1972) Modification of seizure activity by electrical stimulation. II. Motor seizure. *Electroencephalogr Clin Neurophysiol* 32:281–294. [https://doi.org/10.1016/0013-4694\(72\)90177-0](https://doi.org/10.1016/0013-4694(72)90177-0)
- Reddy DS, Kuruba R (2013) Experimental models of status epilepticus and neuronal injury for evaluation of therapeutic interventions. *Int J Mol Sci* 14:18284–18318. <https://doi.org/10.3390/ijms140918284>
- Schafer DP, Lehrman EK, Stevens B (2013) The “quad-partite” synapse: microglia-synapse interactions in the developing and mature CNS. *Glia* 61:24–36. <https://doi.org/10.1002/glia.22389>
- Shibley H, Smith BN (2002) Pilocarpine-induced status epilepticus results in mossy fiber sprouting and spontaneous seizures in C57BL/6 and CD-1 mice. *Epilepsy Res* 49:109–120. [https://doi.org/10.1016/s0920-1211\(02\)00012-8](https://doi.org/10.1016/s0920-1211(02)00012-8)
- Siebold C, Yamashita T, Monnier PP, Mueller BK, Pasterkamp RJ (2017) RGMs: structural insights, molecular regulation, and downstream signaling. *Trends Cell Biol* 27:365–378. <https://doi.org/10.1016/j.tcb.2016.11.009>
- Sirven JI (2015) Epilepsy: a spectrum disorder. *Cold Spring Harb Perspect Med* 5:a022848. <https://doi.org/10.1101/cshperspect.a022848>
- Song M, Tian F, Xia H, Xie Y (2019) Repulsive guidance molecule a suppresses seizures and mossy fiber sprouting via the FAK-p120RasGAP-Ras signaling pathway. *Mol Med Rep* 19:3255–3262. <https://doi.org/10.3892/mmr.2019.9951>
- Sticht C, De La Torre C, Parveen A, Gretz N (2018) miRWalk: an online resource for prediction of microRNA binding sites. *PLoS ONE* 13:e0206239. <https://doi.org/10.1371/journal.pone.0206239>
- Therajaran P, Hamilton JA, O’Brien TJ, Jones NC, Ali I (2020) Microglial polarization in posttraumatic epilepsy: potential mechanism and treatment opportunity. *Epilepsia* 61:203–215. <https://doi.org/10.1111/epi.16424>
- Trinka E, Cock H, Hesdorffer D, Rossetti AO, Scheffer IE, Shinnar S, Shorvon S, Lowenstein DH (2015) A definition and classification of status epilepticus—report of the ILAE task force on classification of status epilepticus. *Epilepsia* 56:1515–1523. <https://doi.org/10.1111/epi.13121>
- Ulrich JD, Ulland TK, Colonna M, Holtzman DM (2017) Elucidating the role of TREM2 in Alzheimer’s disease. *Neuron* 94:237–248. <https://doi.org/10.1016/j.neuron.2017.02.042>
- Upadhy D, Kodali M, Gitai D et al (2019) A model of chronic temporal lobe epilepsy presenting constantly rhythmic and robust spontaneous seizures, co-morbidities and hippocampal neuropathology. *Aging Dis* 10:915–936. <https://doi.org/10.14336/ad.2019.0720>
- Verrotti A, Iapadre G, Di Francesco L, Zagaroli L, Farello G (2020) Diet in the treatment of epilepsy: what we know so far. *Nutrients*. <https://doi.org/10.3390/nu12092645>
- Vezzani A, French J, Bartfai T, Baram TZ (2011) The role of inflammation in epilepsy. *Nat Rev Neurol* 7:31–40. <https://doi.org/10.1038/nrneurol.2010.178>
- Voet S, Prinz M, van Loo G (2019) Microglia in central nervous system inflammation and multiple sclerosis pathology. *Trends Mol Med* 25:112–123. <https://doi.org/10.1016/j.molmed.2018.11.005>
- Walker DG, Lue LF (2015) Immune phenotypes of microglia in human neurodegenerative disease: challenges to detecting microglial polarization in human brains. *Alzheimers Res Ther* 7:56. <https://doi.org/10.1186/s13195-015-0139-9>
- Wang J, Zhao J (2021) MicroRNA dysregulation in epilepsy: from pathogenetic involvement to diagnostic biomarker and therapeutic agent development. *Front Mol Neurosci* 14:650372. <https://doi.org/10.3389/fnmol.2021.650372>
- Wang J, Yu JT, Tan L et al (2015) Genome-wide circulating microRNA expression profiling indicates biomarkers for epilepsy. *Sci Rep* 5:9522. <https://doi.org/10.1038/srep09522>
- Xu X, Gao Y, Shan F, Feng J (2016) A novel role for RGMA in modulation of bone marrow-derived dendritic cells maturation induced by lipopolysaccharide. *Int Immunopharmacol* 33:99–107. <https://doi.org/10.1016/j.intimp.2016.02.008>
- Yu T, Yu H, Zhang B, Wang D, Li B, Zhu J, Zhu W (2019) Promising neuroprotective function for M2 microglia in kainic acid-induced neurotoxicity via the down-regulation of NF-κB and caspase 3 signaling pathways. *Neuroscience* 406:86–96. <https://doi.org/10.1016/j.neuroscience.2019.03.002>

Publisher's Note Springer Nature remains neutral with regard to jurisdictional claims in published maps and institutional affiliations.